

Williams, *Eur. J. Biochem.* **200**, 1 (1991); K.-C. Chang, G. Goldspink, J. Lida, *Arch. Virol.* **110**, 151 (1990).
 7. E. de Clerq, *Antibiot. Chemother. (Basel)* **27**, 251 (1980); I. Gresser, *Cell. Immunol.* **34**, 406 (1977); F. D. Finkelman *et al.*, *J. Exp. Med.* **174**, 1179 (1991).
 8. To construct the Mx-cre expression vector, we ligated a 2.3-kb Eco RI–Bam HI fragment containing the Mx1 gene promoter (5) to the modified coding region of Cre [H. Gu, Y. R. Zou, K. Rajewsky, *Cell* **73**, 1155 (1993)], which includes a nuclear localization signal, and to a 2.1-kb fragment of the human growth hormone gene, which provides splicing and polyadenylation signals [K. E. Chaffin *et al.*, *EMBO J.* **9**, 3821 (1990)]. Transgenic mice were produced by pronucleus injection of fertilized (C57BL/6x CBA)F₂ eggs. Founder mice were first screened for IFN-inducible expression of Cre with the use of peripheral blood lymphocytes. Of 42 strains generated, 16 showed inducible Cre expression and

were crossed to mice harboring the *poβ*^{lox} allele to test for Cre-mediated deletion in vivo. Strains Mx-cre31a and 31b, which contain ~10 transgene copies and originate from the same founder mouse but are distinguished by their transgene integration pattern, showed the most extensive deletion.
 9. The extent of deletion was comparable in purified B cells, T cells, and non-B–non-T cells (11).
 10. These results were reproducible in several independent experiments (R. Kühn, unpublished data).
 11. R. Kühn, unpublished data.
 12. H. Weber, D. Valenzuela, G. Luijber, M. Gubler, C. Weissmann, *EMBO J.* **6**, 591 (1987).
 13. J. Löhler, unpublished data.
 14. Stainings were performed with antibodies to B220, immunoglobulin M, CD3, CD4, and CD8 (R. Kühn, unpublished data).
 15. T. F. Dougherty, *Physiol. Rev.* **32**, 379 (1952).

16. M. G. Whatelet, P. M. Berr, G. A. Huez, *Eur. J. Biochem.* **206**, 901 (1992).
 17. R. K. Singhal and S. H. Wilson, *J. Biol. Chem.* **268**, 15906 (1993); T. S.-F. Wang, *Annu. Rev. Biochem.* **60**, 513 (1991); K. Wiebauer and J. Jiricny, *Proc. Natl. Acad. Sci. U.S.A.* **87**, 5842 (1990).
 18. U. Müller *et al.*, *Science* **264**, 1918 (1994).
 19. We thank J. Löhler for the histological analysis, H. Gu for *poβ* gene-targeted mice, C. Weissmann for IFN, and U. Ringeisen for graphical work. Supported by Deutsche Forschungsgemeinschaft grant SFB 243, the Human Frontier Science Program, the Bundesministerium für Forschung und Technologie, and the Land Nordrhein-Westfalen. F.S. is supported by a stipend from the Boehringer Ingelheim Fonds.

17 May 1995; accepted 18 July 1995

The Chromodomain Protein Swi6: A Key Component at Fission Yeast Centromeres

Karl Ekwall,* Jean-Paul Javerzat,*† Axel Lorentz, Henning Schmidt, Gwen Cranston, Robin Allshire‡

Centromeres attach chromosomes to the spindle during mitosis, thereby ensuring the equal distribution of chromosomes into daughter cells. Transcriptionally silent heterochromatin of unknown function is associated with centromeres in many organisms. In the fission yeast *Schizosaccharomyces pombe*, the silent mating-type loci, centromeres, and telomeres are assembled into silent heterochromatin-like domains. The Swi6 chromodomain protein affects this silencing, and now it is shown that Swi6p localizes with these three chromosomal regions. In cells lacking Swi6p, centromeres lag on the spindle during anaphase and chromosomes are lost at high rates. Thus, Swi6p is located at fission yeast centromeres and is required for their proper function.

Cytologically observable heterochromatin in *Drosophila* and mammals is, in general, incompatible with gene expression (1, 2). The function of these transcriptionally silent regions remains enigmatic (1, 2). Higher eukaryotic centromeres, with their associated kinetochore complex, are formed in the vicinity of centromeric heterochromatin, but whether heterochromatin itself contributes to centromere function is unknown. One possibility is that transcriptional repression at centromeres, and therefore heterochromatin, is a manifestation of normal centromere-kinetochore assembly. If this is true, then certain gene products should localize with centromeres and play a role in both the formation of silent heterochromatin and centromere function.

In the fruit fly *Drosophila melanogaster* and in mammals, proteins containing chromodo-

main, a motif first described as a region of similarity between HP-1 and *Polycomb* (3), are associated with heterochromatin or impose repression in a temporal manner on important developmental genes (4–10). Mutations in the *Drosophila* gene *Su(var)205*, which encodes the chromodomain protein HP-1, were originally identified as suppressors of variegating position effects, which suggested a role for HP-1 in the formation of heterochromatin (11). In the fission yeast *Schizosaccharomyces pombe*, the silent mating-type loci, centromeres, and telomeres share several properties with heterochromatin domains (12–14). The *swi6*⁺ gene of fission yeast encodes a chromodomain protein and is required to maintain transcriptional

repression at the silent mating-type loci and centromeres (15, 16). Mutations in the *swi6* gene result in a highly increased rate of chromosome loss (16). The chromodomain of Swi6p is 46% identical to that of *Drosophila* HP-1 across this 50-amino acid domain (15). We now present evidence that the Swi6 protein is an important functional component at fission yeast centromeres.

A purified fusion protein was used to raise a polyclonal serum and to affinity-purify Swi6p-specific antibodies (anti-Swi6p). Protein immunoblotting with anti-Swi6p detected a single band migrating at ~50 kD in extracts from wild-type strains (Fig. 1A) (17). This band was absent in extracts from strains in which the *swi6*⁺ gene is deleted (*swi6::his1*), and only a faint signal was seen in extracts from strains with the missense *swi6-115* allele (W269R).

Immunofluorescence analysis with affinity-purified anti-Swi6p produced a distinct pattern of staining in fixed cells (17). Several discrete spots were seen in interphase haploid and diploid cells (red, Fig. 1, B and C). Most haploid and diploid cells contained three and five spots of anti-Swi6p fluorescence, respectively (Fig. 1E). No staining with anti-Swi6p was detected in strains harboring a complete deletion of the *swi6* gene (Fig. 1D).

Mutations at *swi6* cause a high rate of chromosome loss during mitosis (Table 1) and affect silencing within the centromere (16). It therefore seemed plausible that some of the anti-Swi6p spots might repre-

Table 1. Frequency of chromosome lagging and loss in wild-type and *swi6* mutants at 18°C.

Back-ground	Cells in late anaphase (%) [*]	Late anaphase cells with lagging centromeres (%) [*]	Rate of minichromosome loss (Ch16) per division [†]
Wild type	3.5	<1.0 (0/98)	<0.08 (0/1241)
<i>swi6::his</i> ⁺	3.7	48.8 (39/80)	4.6 (17/370)
<i>swi6-115</i>	2.7	24.5 (15/61)	1.3 (11/849)

*These authors contributed equally to this work.

†Present address: Laboratoire de Génétique, Université de Bordeaux II, Avenue de Facultés, 33405 Talence, France.

‡To whom correspondence should be addressed.

*Late anaphase cells were defined as cells with a spindle length greater than 5 μm. Cells were classified as having lagging centromeres if a single centromere FISH signal was detected at least 1.5 μm away from an anaphase spindle pole (as in Fig. 4B). For all strains, the frequency of lagging centromeres and minichromosome loss were measured in cells from the same culture. Similar results were obtained in different cultures. †The rate of minichromosome loss was determined as described (16).

sent fission yeast centromeres. To investigate this possibility, we stained wild-type, diploid cells with anti-Swi6p and then de-

tected centromeres by fluorescent in situ hybridization (FISH) (18, 19). In interphase cells (Fig. 1), between three and six

spots of staining (red, Fig. 2A) were detected, one of which (generally the largest) colocalized with the centromere FISH signal (green, Fig. 2A; colocalization of red with green produces yellow in the merged image, top left). In interphase fission yeast cells, all centromeres aggregate at the nuclear periphery adjacent to the spindle pole body (19). Thus, in diploid cells at G2 interphase, a single large spot of centromere staining was expected even though these cells contained 12 copies of centromeric DNA.

In addition to the large centromeric anti-Swi6p-stained spot, several smaller spots were detected that varied in number from two to six when all focal planes of cells were examined. Fission yeast telomeres cluster at the nuclear periphery, and during G2 in diploids the number of spots detected by FISH with the telomere Cos212 probe is in the range of one to five (19). The Cos212 probe was used to detect the telomeres of chromosomes 1 and 2 (green, Fig. 2B) in anti-Swi6p-stained cells (red, Fig. 2B). In the five cells shown, the telomere signals colocalized with spots of anti-Swi6p staining (yellow in merged image, Fig. 2B, top left). All cells contained a large anti-Swi6p-stained spot that did not coincide with the

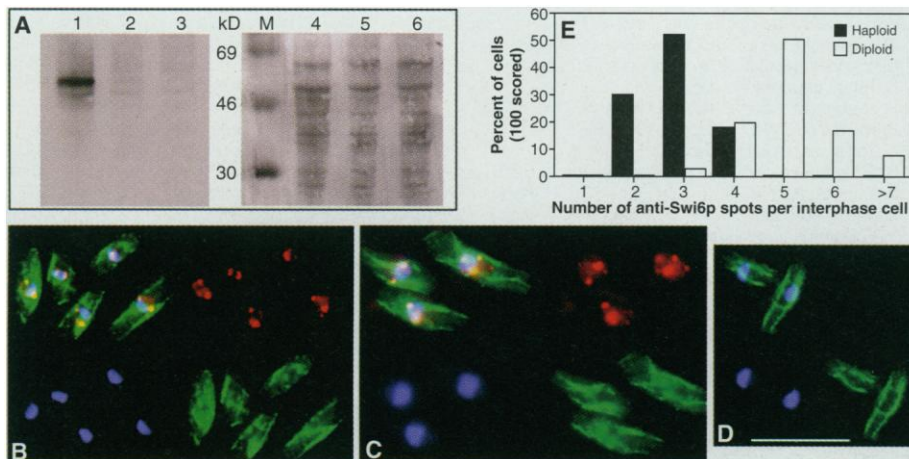


Fig. 1. Generation of antiserum to Swi6p. **(A)** Immunoblot of total protein extracted from wild-type (lanes 1 and 4), *swi6-115* (lanes 2 and 5), and *swi6::his1* (lanes 3 and 6) strains was probed with affinity-purified anti-Swi6pR4 (lanes 1 to 3) and counterstained with amido black to compare loading (lanes 4 to 6) (17). A single band migrating at 50 kD is apparent in wild-type but not in deletion strains. **(B to D)** Wild-type haploid and diploid cells and *swi6::his1* cells, respectively, fixed and stained with affinity-purified anti-Swi6p (red), mouse anti-tubulin TAT1 monoclonal antibody (green), and DAPI, which stains chromosomal DNA (blue) (17). The merged three-color image is shown at the top left of (B), (C), and (D). **(E)** Distribution of haploid and diploid cells with various numbers of anti-Swi6p spots. Images (B, C, and D) are at the same magnification. Bar in (D), 10 μ m.

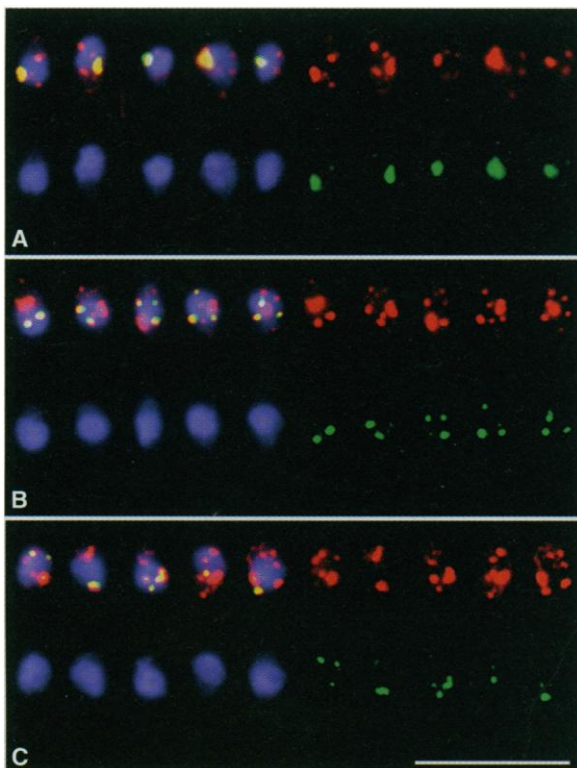
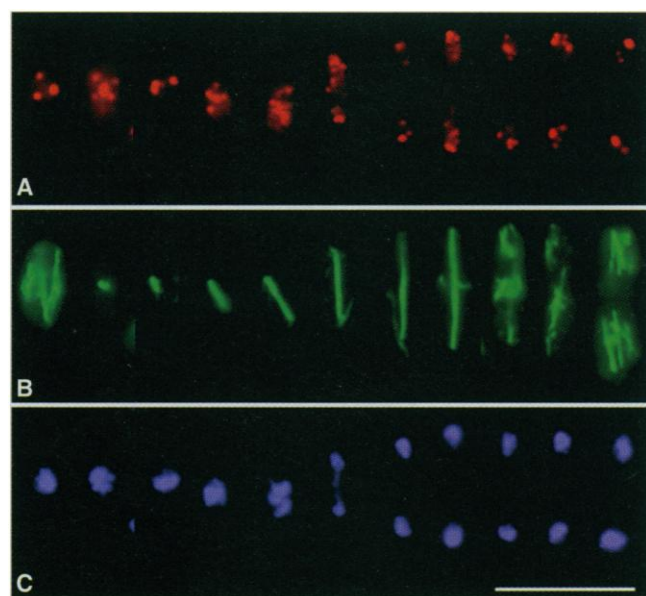


Fig. 2 (left). Colocalization of Swi6 protein with centromeres, telomeres, and the mating-type loci. Montages of wild-type diploid cells stained with anti-Swi6p (red) and the digoxigenin-labeled probes (green). **(A)** Centromeric DNA (pRS140) (19), **(B)** telomere-associated DNA (Cos212) (19), and **(C)** mating-type loci DNA (pON6, 7, and 8) (25). DAPI staining is shown in blue. In (A), (B), and (C) the merged, three-color image is shown at the top left where yellow is produced upon colocalization of red (Swi6p) and green



(FISH) signals. Bar, 10 μ m. **Fig. 3 (right).** Localization of Swi6 protein through the fission yeast cell cycle. Wild-type haploid cells were stained with affinity-purified anti-Swi6p **(A)**, red, mouse anti-tubulin TAT1 monoclonal antibody as a marker for stages through the cell cycle **(B)**, green, and DAPI **(C)**, blue (17, 20). For each cell, the corresponding panels are placed below each other. From left to right, an example is shown of a cell at various stages of the cell cycle passing from interphase through the equivalent of metaphase, anaphase, telophase, and cytokinesis. The brightest spots represent the centromeres, which in early mitosis cluster in the center of the short spindle and then move toward the poles. Upon spindle elongation, the centromere spots remain in close proximity to the poles, while the remaining spots (telomeres and *mat* loci) trail toward the center of the spindle. Upon septum formation (cytokinesis), an interphase arrangement is reestablished. Cells were fixed and stained as described (17). Bar, 10 μ m.

telomere signal; from the data shown in Fig. 2A, it is likely that this large spot represents the centromeres. Remaining anti-Swi6p signals could represent the telomeres of chromosome 3, which lack telomere-associated repeats (19), or the silent mating-type loci. The same h^{+N} diploid cells stained with anti-Swi6p were also subjected to FISH with a probe for the mating-type loci (Fig. 2C) (18). One to two major signals were detected with this *mat* locus probe (green), which colocalized with anti-Swi6p spots (red) in the merged image (yellow, top left).

A series of images are shown (Fig. 3) of wild-type, haploid cells stained with anti-Swi6p (red) and anti-tubulin (green) (17), to mark the stages of the cell cycle from interphase through mitosis (20). The anti-Swi6p staining was present on the chromosomes during mitosis and followed the same dynamics as reported for centromeres and telomeres throughout the cell cycle (19).

Mutation or deletion of the *swi6* gene resulted in a 30- to 100-fold increase in the rate of chromosome loss (Table 1) (16). To assess the nature of these chromosome segregation defects in strains bearing the null allele, we analyzed fixed cells by staining with anti-tubulin (green, Fig. 4) to indicate their position in the cell cycle and then subjected the cells to FISH with a centromere probe (red, Fig. 4) (21). Late anaphase cells, with spindle lengths greater than 5 μm , represented 3.7% of the population in asynchronous log phase cultures of wild-type strains (Table 1). At this stage, the centromeres and chromosomes had completed segregation and were located at the poles of these spindles in all cells (Fig. 4A and Table 1). In contrast, in cells with no *swi6* gene, a high incidence (48.8%) of lagging centromeres was detected (Fig. 4B and Table 1). Aberrant segregation events were also detected in the *swi6-115* mutant (Table 1). Defective centromere function in *swi6* mutants is presumably a consequence of the absence of this protein at centromeres, which results in the assembly of weakened kinetochores. These kinetochores must be defective in their interaction with microtubules so that the chromosomes move more slowly to the poles during anaphase.

These data demonstrate that the Swi6 protein is localized to all three heterochromatin-like regions of the fission yeast nucleus, including the centromere. There are similarities between the roles of Swi6p in *S. pombe* and HP-1 in *Drosophila*. HP-1 localizes at pericentric heterochromatin (7, 10) and is involved in the unstable repression imposed on genes placed adjacent to heterochromatin (4). Homozygous mutants in HP-1 are late larval lethal, and the affected larvae display a high incidence of defects in chromosome segregation (22). Mutations at the *swi6* locus affect transcriptional silencing at the centromere (16), cause a high frequency of lagging centromeres during late anaphase, and have highly increased rates of chromosome loss. In addition, the Swi6 protein is associated with the centromere. One major difference between the phenotype of fission yeast *swi6* and *Drosophila* HP-1 mutants is that in the latter, centromere movement to the spindle pole during anaphase is unaffected and the primary defect appears to be in chromosome condensation, whereas the *swi6* mutations affect the ability of centromeres to migrate to the poles of the spindle during anaphase. This observation is consistent with the Swi6 protein being an integral functional component at fission yeast centromeres, the assembly of which mediates the formation of a heterochromatin-like repressive structure.

These data demonstrate that the Swi6 protein is localized to all three heterochromatin-like regions of the fission yeast nucleus, including the centromere. There are similarities between the roles of Swi6p in *S. pombe* and HP-1 in *Drosophila*. HP-1 localizes at pericentric heterochromatin (7, 10) and is involved in the unstable repression imposed on genes placed adjacent to heterochromatin (4). Homozygous mutants in HP-1 are late larval lethal, and the affected larvae display a high incidence of defects in chromosome segregation (22). Mutations at the *swi6* locus affect transcriptional silencing at the centromere (16), cause a high frequency of lagging centromeres during late anaphase, and have highly increased rates of chromosome loss. In addition, the Swi6 protein is associated with the centromere. One major difference between the phenotype of fission yeast *swi6* and *Drosophila* HP-1 mutants is that in the latter, centromere movement to the spindle pole during anaphase is unaffected and the primary defect appears to be in chromosome condensation, whereas the *swi6* mutations affect the ability of centromeres to migrate to the poles of the spindle during anaphase. This observation is consistent with the Swi6 protein being an integral functional component at fission yeast centromeres, the assembly of which mediates the formation of a heterochromatin-like repressive structure.

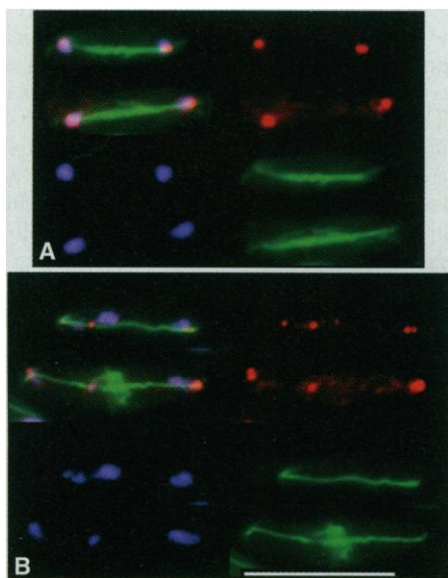


Fig. 4. Lagging centromeres and chromosomes in anaphase of *swi6* mutants. Late anaphase wild-type haploid (A) and *swi6::his1* (B) cells stained with anti-tubulin TAT1 monoclonal antibody as a marker for cell cycle stage as related to spindle appearance and length (green) (17, 20), the digoxigenin-labeled centromeric DNA probe (red) (21), and DAPI (blue). The three-color merged image is shown at the top left of (A) and (B). Only in cells lacking the Swi6 protein (*swi6::his1*) are centromeres (red spots) observed to lag on anaphase spindles (see Table 1). In many of these cells, lagging chromosomes can also be seen by DAPI staining in blue (B). Bar, 10 μm .

REFERENCES AND NOTES

1. S. Henikoff, *Trends Genet.* **6**, 422 (1990).
2. G. Karpen, *Curr. Opin. Genet. Dev.* **4**, 281 (1994).
3. R. Paro and D. S. Hogness, *Proc. Natl. Acad. Sci. U.S.A.* **88**, 263 (1991).
4. J. C. Eissenberg, G. D. Morris, G. Reuter, T. Hartnett, *Genetics* **131**, 345 (1992).
5. K. A. Wreggett *et al.*, *Cytogenet. Cell Genet.* **66**, 99 (1994).
6. W. S. Saunders *et al.*, *J. Cell Sci.* **104**, 573 (1993).
7. J. A. Powers and J. C. Eissenberg, *J. Cell Biol.* **120**, 291 (1993).
8. S. Messmer, A. Franke, R. Paro, *Genes Dev.* **6**, 1241 (1992).
9. R. Paro, *Curr. Opin. Cell Biol.* **5**, 999 (1993).
10. R. Kellum, J. W. Raff, B. M. Alberts, *J. Cell Sci.* **108**, 1407 (1995).
11. J. C. Eissenberg *et al.*, *Proc. Natl. Acad. Sci. U.S.A.* **87**, 9923 (1990).
12. A. J. S. Klar, *Trends Genet.* **8**, 208 (1992).
13. R. C. Allshire, J. P. Javerzat, N. J. Redhead, G. Cranston, *Cell* **76**, 157 (1994).
14. E. R. Nimmo, G. Cranston, R. C. Allshire, *EMBO J.* **13**, 3801 (1994).
15. A. Lorentz, K. Ostermann, O. Fleck, H. Schmidt, *Gene* **143**, 139 (1994).
16. R. C. Allshire, E. R. Nimmo, K. Ekwall, J. P. Javerzat, G. Cranston, *Genes Dev.* **9**, 218 (1995).
17. Amino acids 11 to 328 of Swi6p were fused in frame with the HisX6-tag by cloning a HinPI-NsiI fragment of the genomic clone pAL2 (15) between the BstBI and HindIII sites of pRSETA (Invitrogen). Upon induction, a protein migrating at ~50 kD was produced. Native Swi6 fusion protein was purified by passing extract over a Ni²⁺-agarose column (Probond-Invitrogen) and eluted with 0.2 to 0.5 M imidazole. Fusion protein was dialyzed and concentrated on a Centricon 30 (Amicon) emulsified with Titremax (Hunter's) and injected into rabbits. Affinity purification was done as described (24). For fixation, all cells were grown to $\sim 5 \times 10^6$ cells per milliliter in yeast extract supplemented (YES) at 18°C, and an equal volume of YES + 2.4 M sorbitol was added for 10 min before the addition of paraformaldehyde to a final concentration of 3.8%. Cells were incubated for 30 to 45 min and then treated as described (20). Fixed cells were incubated with mouse anti-tubulin TAT1 monoclonal antibody (23) and affinity-purified anti-Swi6pR4 at a 1/15 dilution overnight in PEMBAL (20). After extensive washing, cells were incubated overnight with fluorescein isothiocyanate-conjugated antimouse immunoglobulin G (IgG) (Sigma) and CY3-conjugated anti-rabbit IgG (Sigma) at a 1/100 dilution in PEMBAL. Cells were washed, stained with DAPI, and mounted as described (20) in Vectashield mountant (Vector Labs). Cells were observed with a Zeiss Axioplan fluorescence microscope and images captured with a Photometrics charge-coupled device camera and manipulated with IP LAB Spectrum/Digital Scientific Software.
18. Cells were fixed and stained with affinity-purified anti-Swi6p (17) and were then refixed, denatured, and hybridized with labeled probe as described (19). The DNA probes were labeled with digoxigenin-11-deoxyuridine triphosphate by nick translation.
19. H. Funabiki, I. Hagan, S. Uzawa, M. Yanagida, *J. Cell Biol.* **121**, 961 (1993).
20. I. M. Hagan and J. S. Hyams, *J. Cell Sci.* **89**, 343 (1988).
21. Cells were fixed and stained as described (17, 18) except that the digoxigenin-labeled probe was detected by incubation with rhodamine-conjugated anti-digoxigenin antibodies raised in sheep (Vector Labs).
22. R. Kellum and B. Alberts, *J. Cell. Sci.* **108**, 1419 (1995).
23. A. Woods *et al.*, *ibid.* **93**, 491 (1989).
24. D. E. Smith and P. A. Fisher, *J. Cell Biol.* **99**, 20 (1984).
25. D. H. Beach, *Nature* **305**, 682 (1983).
26. We thank members of the Chromosome Biology Section and W. Bickmore, I. Hagan, N. Hastie, and R. Meehan for discussion and comments on the manuscript. We also thank J. Fantes, W. Bickmore, and P. Perry for help with FISH and microscopy and N. Davidson, S. Bruce, and D. Stuart for the art work. We are indebted to I. Hagan for expert advice on cell fixation and immunofluorescence and H. Funabiki and M. Yanagida for teaching R.A. the FISH technique and for providing probes. We are grateful to K. Gull for supplying the TAT1 monoclonal antibody. K.E. was funded by the European Molecular Biology Organization and is the recipient of a Human Frontier Science Program fellowship. J.-P.J. was funded by Wellcome and European Union Human Capital and Mobility Program fellowships. Supported by the Medical Research Council of Great Britain.

19 April 1995; accepted 28 June 1995